AMSE JOURNALS-2016-Series: Advances C; Vol. 71; N°1; pp 39-59

Submitted June 2016; Revised Sept. 15, 2016, Accepted Oct. 15, 2016

Robust H_∞ Loop Shaping Controller for Load Frequency Control of an Uncertain Deregulated Power System

*Arlene Davidson R, **S. Ushakumari

*Department of Electrical Engineering, College of Engineering,

Trivandrum, Kerala, India (arlenerosaline1@gmail.com)

**Department of Electrical Engineering, College of Engineering

Trivandrum, Kerala, India, (ushalal2002@gmail.com)

Abstract

Load frequency control forms an essential component of Automatic Generation Control, which helps to maintain the power system frequency constant while maintaining the tie-line power flow with neighbouring áreas at scheduled values for an interconnected power system. With deregulation, the structure of electric power industry is changed thoroughly with multiple bilateral transactions taking place in a competitive market environment. In the changed scenario, the conventional controllers are no more capable of satisfying the control requirements. Hence, robust controllers are suggested for load frequency control which can handle the uncertainties that are rampant in the system. In this paper, a robust H_∞ loop shaping controller is used as load frequency controller for a two área deregulated power system with non-reheat thermal power plants. Analysis of the system performance is done for all contract cases relevant to deregulated power systems. The system behaviour towards different cost functions is also investigated to demonstrate the robustness of the controller.

Key words

Deregulation, contract, unilateral, bilateral, contract violation, loop shaping

1. Introduction

The frequency of an electric power system is a significant indicator of the health of the system since it symbolizes the load-generation balance. Load Frequency Control (LFC) forms an essential component of Automatic Generation Control (AGC) in power systems [1]. The functions of LFC in an interconnected power system include maintaining power system

frequency at nominal value and also maintaining tie-line power flow with neighbouring control areas as per scheduled values. With restructuring taking place globally in power industry, focus has shifted to the challenges facing LFC in the changed situation. Deregulation brings about a horizontally integrated architecture for electric power industry in comparison with the previous vertically integrated one. A deregulated power system structure comprises of GENCOs (Generation Companies), TRANSCOs (Transmission Companies) and DISCOs (Distribution Companies) performing the functions of generation, transmission and distribution respectively with open access policy. In the changed structure, GENCOs may or may not participate in LFC and it is the DISCOs who make contract for power with GENCOs [2]. To ensure power system stability and reliability, the transactions between the GENCOs and DISCOs are monitored by the Independent System Operator (ISO). Several ancillary services including AGC, are controlled by the ISO. Literature survey on LFC in deregulated power system shows that several research works have been done in this area. The different operational structures resulting from deregulation are described in [3] while in [4], a ramp following controller in a deregulated environment is given. A successful method of modelling the several contracts taking place is given in [5] while a robust controller through mixed H_2/H_∞ is described in [6]. A controller based on neural networks is suggested through [7] and an integral controller whose gains are tuned through genetic algorithm optimization is given in [8]. A fuzzy load frequency controller for a restructured power system is given in [9]. Genetic algorithm optimization technique finds application in tuning the PID controller gains in [10]. Optimal output feedback and reduced order techniques are used for LFC in [11]. Internal model control method is used for tuning decentralized PID controller parameters in [12]. Structured singular value analysis of a deregulated system with LFC is given in [13]. Fractional order PID controller for LFC is given in [14] while [15] gives the design of optimal output feedback controller.

A review of the literature pertaining to LFC of deregulated power system shows that the work on robust controllers is minimal. The dynamics of the system indicate that the practical deregulated power system is highly complex with nonlinearities and uncertainty due to multiple bilateral transactions. Hence LFC demands the application of robust controllers rather than conventional controllers which are fixed controllers. The authors have designed an integral controller based on genetic algorithm for a two area deregulated thermal power system [20]. This paper is a work aimed at the design of robust controller for load frequency control of a two area deregulated thermal power system consisting of non-reheat thermal generators [21]. The method of design is that of H_∞ robust loopshaping type controller which is based on the method of

normalized coprime factors [17]. Details of Modelling of the deregulated power system, design and application of H-infinity controller design based on loop-shaping for the system, Simulation Results, Discussions and conclusions are given in Sections 2, 3, 4 and 5 respectively.

2. Modelling of a two area Deregulated Power System

Model of a two area deregulated power system is made such that all possible transactions in the electric power market are taken into account. The transactions include unilateral, bilateral and a combination of these [2]. Unilateral or Poolco type transactions are used to signify the situation where LFC of a control area is done by GENCOs within the same control area. Bilateral transactions signify the power contracts made by DISCOs with GENCOs in any control area. Contract violation is a term identified with the situation where a demand is made by a DISCO in excess of the contracted value. This situation is taken care of by GENCOs in the area in which excess demand occurs [4]. The modelling is done as per the guidelines given by Donde et al [4]. The contracts are represented using a matrix termed as 'DISCO Participation Matrix' (DPM) in which the number of rows is equal to the number of GENCOs and the number of columns is equal to the number of DISCOs. Each element of the matrix designated as 'cpf_{kl}' is called as contract participation factor and its value is computed as the fraction of the total load contracted by the l^{th} DISCO with the k^{th} GENCO. The sum of all elements in a column of the DPM is unity. For a two area system with two GENCOs (GENCO 1 and GENCO 2) and two DISCOs (DISCO 1 and DISCO 2) in 'Area 1' and two GENCOs (GENCO 3 and GENCO 4) and two DISCOs (DISCO 3 and DISCO 4) in 'Area 2', the structure of the DPM is given below.

$$\begin{bmatrix} cpf_{11} & cpf_{12} & cpf_{13} & cpf_{14} \\ cpf_{21} & cpf_{22} & cpf_{23} & cpf_{24} \\ cpf_{31} & cpf_{32} & cpf_{33} & cpf_{34} \\ cpf_{41} & cpf_{42} & cpf_{43} & cpf_{44} \end{bmatrix} \quad (1)$$

where

$$\sum_{k=1}^{Ng} cpf_{kl} = 1; \text{ for } l = 1,2,.....N_d \quad (2)$$

Where, '*Ng*' is the total number of GENCOs and 'N_d' the total number of DISCOs. The schematic block diagram for load frequency control of such a power system is given in fig.1. The generation of each GENCO must track the contracted demands of DISCOs in steady state. The expression for contracted power of k^{th} GENCO with DISCOs is given by

$$\Delta P_{gc,k} = \sum_{l=1}^{Nd} cpf_{kl} \Delta P_{L,l}; \text{ for } k = 1,2,.....Ng \quad (3)$$

Where, $\Delta P_{gc,k}$ is the contracted power of k[th] GENCO and $\Delta P_{L,l}$ is the total load demand of l^{th} DISCO. The scheduled steady state power flow on the tie-line is expressed as the difference of total power exported from GENCOs in control area 1 to DISCOs in control area 2 and total power imported by DISCOs in control area 1 from GENCOs in control area 2.

$$\Delta Ptie_{12,scheduled} = \sum_{k=1}^{2}\sum_{l=3}^{4} cpf_{kl}\,\Delta P_{L,l} - \sum_{k=3}^{4}\sum_{l=1}^{2} cpf_{kl}\,\Delta P_{L,l} \quad (4)$$

$$\Delta Ptie_{12,error} = \Delta Ptie_{12,actual} - \Delta Ptie_{12,scheduled} \quad (5)$$

At steady state, tie-line power error, $\Delta Ptie_{12,error}$ vanishes as the actual tie-line power flow reaches the scheduled power flow. This error signal is used to generate the respective Area Control Error (ACE) signal as in the conventional power system.

$$ACE_1 = B_1\Delta f_1 + \Delta Ptie_{12,error} \quad (6)$$

$$ACE_2 = B_2\Delta f_2 + a_{12}\Delta Ptie_{12,error} \quad (7)$$

where $a_{12} = -\frac{Pr1}{Pr2}$ where P_{r1}, P_{r2} are the rated area capacities of area 1 and area 2 respectively.

The total load of the k[th] control area $\Delta P_{d,k}$ is expressed as the sum of the contracted and uncontracted load demand of the DISCOs of the k[th] control area.

$$\Delta P_{d,k} = \sum_{k=1}^{Nd}\Delta P_{L,k} + \Delta P_{UL,k} \quad (8)$$

where, $\Delta P_{L,k}$ is the contracted load demand of the k[th] DISCO and $\Delta P_{UL,k}$ represents the uncontracted load demands of DISCOs in k[th] area.

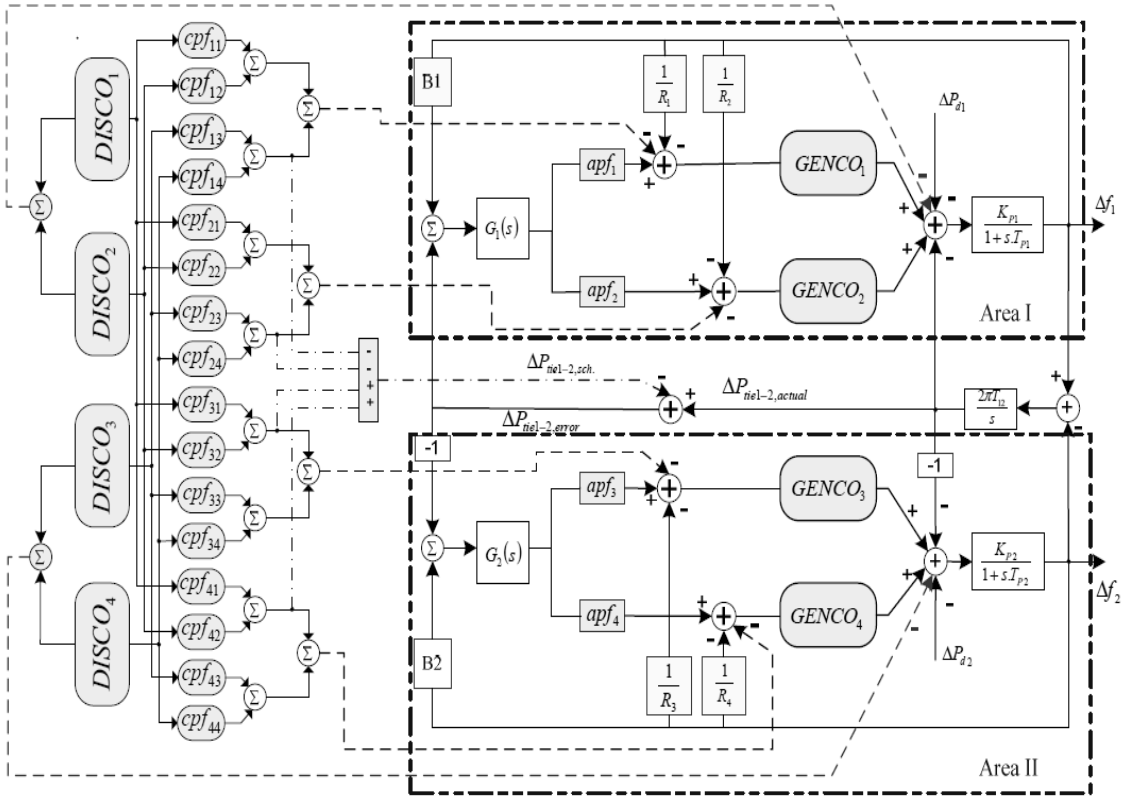

Fig. 1. Schematic block diagram of a deregulated power system

3. Load frequency control in deregulated environment

The deregulated power system operates in a free market environment. It is the DISCOs who make contract for power with the GENCOs. There are several market structures in deregulated power systems throughout the world, but the salient features of the transactions involved include (1) Unilateral or Poolco type transactions (2) Bilateral transactions or a combination of (1) and (2) [3]. Unilateral type of transactions are the transactions existing between DISCOs and GENCOs within the same área. Bilateral transactions are the transactions between DISCOs and GENCOs in any control área.

3.1. Design of H_∞ Loopshaping Controller

The design of load frequency controller in a deregulated environment should be such as to accommodate different kinds of transactions possible. Thus practically, we can see that a conventional controller may not be able to handle the risks associated with the large volume of transactions taking place. This is because a fixed controller design is done based on the plant

model corresponding to a particular load-demand combination. Hence we see the necessity of a robust controller which would take care of the uncertainties in the plant model considering the nature of bilateral transactions.

Objectives of robust controller synthesis include ensuring the stability of systems in the face of uncertainties in the system referred to as robust stability. In the control design for uncertain systems, it is necessary to know the level of performance once stability is ensured. This is called as robust performance. The term 'loop-shaping' refers to adjustment of frequency response of whole system within certain bounds so as to ensure sufficient robust performance and robust stability [19].

Consider $G_i(s)$ as a linear time invariant model for a given control area i

$$\dot{X}_i = A_i X_i + B_{1i} w_i + B_{2i} u_i \quad (9.1)$$

$$z_i = C_{1i} X_i + D_{12i} u_i \quad (9.2)$$

$$y_i = C_{2i} X_i \quad (9.3)$$

Where X_i is the state variable vector, w_i is the disturbance vector, z_i is the controlled output vector and y_i is the measured output vector performed by ACE signal. The H_∞ controller for the linear time invariant system $G_i(s)$ with the state space realization given in (9.1-9.3) is to find a matrix K, given by $u = Ky_i$, such that the resulting closed loop system is internally stable and the H_∞ norm from w to z is smaller than γ, a specified positive number, ie.,

$$\|T_{zw}\|_\infty < \gamma \quad (10)$$

Solution to obtain H infinity controller through Riccati equations are found in Zhou *et. al* [19]. These methods suggest weights to be suitably inserted along with the plant model to get a predefined performance. Fig. 2 shows the generalized closed loop model of a plant P(s) with controller K(s), the weights W_e, W_p are used to specify the closed loop transfer function; W_u indicates the restriction on u, W_i, W_o, W_n are used to model disturbances and noise; W_r models the reference.

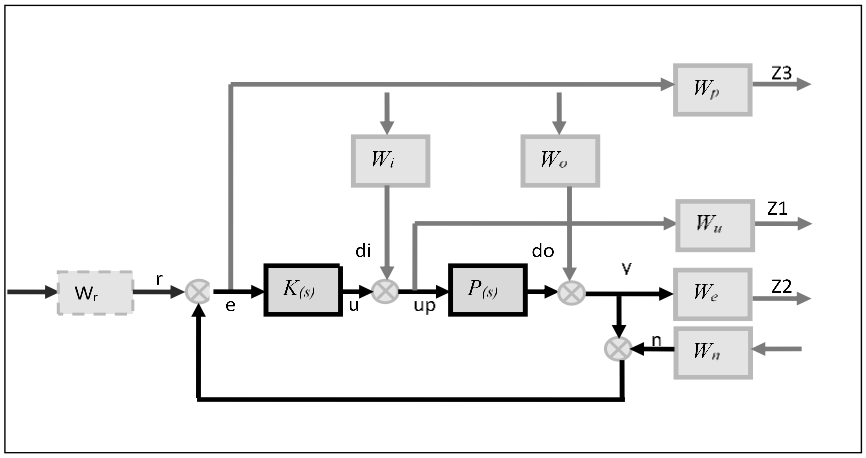

Fig. 2. Framework of Conventional H∞ Controller Design

Above method is cumbersome because the weights have to be adjusted by a trial and error process.

H∞ norm is defined as the supremum of the largest singular value over all frequencies. For a stable matrix transfer function G(s), the H∞ norm of G(s) can be regarded as the largest possible amplification factor of the system's steady state response to sinusoidal excitations. It also appears as the peak value on the Bode magnitude plot of $|G(j\omega)|$. Graphically, the infinite norm of a transfer function is obtained as the peak value of a Bode singular value plot. In loop-shaping method of H∞ controller synthesis [17], closed-loop objectives are specified in terms of requirements on open-loop singular values. This method is different from conventional H∞ design in that robust stabilization is done without frequency weighting. Also, loop-shaping is done here without explicitly considering nominal plant phase information. Desired closed-loop performance is achieved by selecting a controller which provides sufficiently high open-loop gain at low frequency (where modelling error is low) and robust stability is ensured by having a controller which provides sufficiently low open-loop gain at high frequency (where modelling error is high).

For a given plant G and controller K, the closed-loop performance objectives are given by

A. $\bar{\sigma}(I + GK)^{-1}$ termed Sensitivity, 'S' which is the gain from output disturbance to controller input, or the gain from reference signal to tracking error.

B. $\bar{\sigma}((I + GK)^{-1}G)$, which is the transfer function from input disturbance to plant output. The reciprocal of this term indicates the maximum permissible additive controller perturbation for closed-loop stability.

C. $\bar{\sigma}(K(I+GK)^{-1})$ which is the transfer function from output disturbance to controller output. The reciprocal of this term represents the maximum allowable additive plant perturbation for closed-loop stability.

D. $\bar{\sigma}(GK(I+GK)^{-1})$ termed 'Complementary Sensitivity, T' which is the transfer function from controller input disturbance to plant output and also the same as transfer function from control input to output. The reciprocal of this term represents the maximum permissible multiplicative plant perturbation for closed-loop stability. A. and B. are closed-loop performance objectives and are particularly significant at low frequency while C. and D. are robust stability objectives which are required to be small at high frequency. According to the mentioned properties, open loop singular value shaping is done. This can be illustrated as in fig. 3. Here a target loop-shape is selected (thick line in fig. 3) based on the following criteria.

1. For stability robustness, the target loop-shape should have low gain at high frequencies
2. For performance, the desired loop-shape should have high loop-gain at low frequencies to ensure good control accuracy and disturbance attenuation.
3. Desired loop-gain should have its 0 dB crossover frequency, ω_c, between the above two frequency ranges and below ω_c, it should roll-off with a negative slope between -20 dB/decade and -40 dB/decade which helps to keep phase lag to less than -180^0 inside control loop bandwidth ($0<\omega<\omega_c$)
4. The 0 dB crossover frequency should be more than the magnitude of any right half plane poles of the plant and less than the magnitude of any right half plane zeroes of the plant.

Unstructured uncertainty in the plant is represented using coprime factor perturbations.

If the nominal plant is given by

$$G = \widetilde{M}^{-1}\widetilde{N} \tag{11}$$

then a perturbed plant is written as

$$G_\Delta = \left(\widetilde{M} + \Delta_M\right)^{-1}\left(\widetilde{N} + \Delta_N\right) \tag{12}$$

where $\widetilde{M}, \widetilde{N}$ is a left coprime factorization of G and

Δ_M, Δ_N are stable, unknown transfer functions representing uncertainty and satisfying $\|(\Delta_M, \Delta_N)\|_\infty < \epsilon > 0$.

The design objective is then to design a feedback controller K which stabilizes all such G_Δ for a given $\in$. The same can be expressed in terms of H_∞ norm optimization.ie., to find a stabilizing controller K which satisfies

$$\left\| \begin{bmatrix} (I+GK)^{-1}(\tilde{M})^{-1} \\ K(I+GK)^{-1}(\tilde{M})^{-1} \end{bmatrix} \right\|_\infty \leq \epsilon^{-1} \tag{13}$$

It is seen from [17] that the maximum value of $\in$ is given by $\in_{max}$

$$= 1 - \left(\left\| [\tilde{M}, \tilde{N}] \right\|_H^2 \right)^{1/2} \tag{14}$$

Where, the suffix H for the above norm indicates Hankel norm and $\in_{max}$ is called the maximum stability margin. A stabilizing controller which achieves $\in = \in_{max}$ is called an optimal controller and a controller which achieves $\in < \in_{max}$ is called suboptimal controller.

The loop-shaping design procedure is listed below:

1. Choose a desired loop-shape whose transfer function is given by G_d whose performance bound and robustness bound are as in fig. 3.

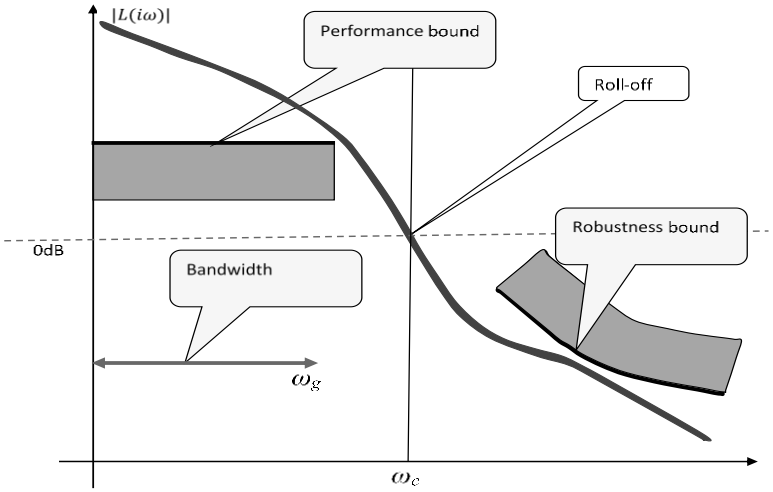

Fig. 3. Desired loop-shape in Loop-shaping

2. Conversion of G_d to the form in which the singular values of the nominal plant are shaped to give the desired open-loop shape. The shaped plant can be expressed as $G_d=W_2GW_1$, where W_1 is a pre-compensator and W_2 is a post-compensator. Here W_1 could be assumed unity for simplification. Methods for achieving the same are given in [16] and [18].

3. Calculate ϵ_{max} using

$$\epsilon_{max}^{-1} \triangleq \inf_{K \text{ stabilizing}} \left\| \begin{bmatrix} I \\ K \end{bmatrix} (I + G_d K)^{-1} \tilde{M}_S^{-1} \right\|_\infty \quad (15)$$

where $\tilde{M}_s$ and $\tilde{N}_s$ define the normalized coprime factors of G_d.

If $\epsilon_{max} << 1$, return to 1 and adjust W_1 and W_2. Select $\epsilon \lesssim \epsilon_{max}$ and synthesise controller which satisfies

$$\left\| \begin{bmatrix} I \\ K_\infty \end{bmatrix} (I + G_d K_\infty)^{-1} \tilde{M}_S^{-1} \right\|_\infty \leq \epsilon^{-1} \triangleq \gamma \quad (16)$$

The final feedback controller is constructed by combining H_∞ controller K_∞ with the shaping functions W_1 and W_2 such that $K = W_1 K_\infty W_2$.

The value of γ directly determines the frequency range over which loop-shaping is valid. So a small γ indicates that the achieved loopshape differs from the specified loopshape by only a limited amount. It can be shown [17] that for any $\epsilon \lesssim \epsilon_{max}$, there will be a minimum deterioration in the desired loop-shape at frequencies of high or low loop-gain.

For the two-area deregulated power system having two GENCOs and two DISCOs in each area (Fig. 1) in which the GENCOs are assumed to be non-reheat thermal type, whose parameters are mentioned in Appendix A, the above loop-shaping method was applied using the Robust Control Toolbox in Matlab [22]. The state space model of the two area deregulated power system is given in Appendix B. The target loop-shape was selected as G_d=1/s for both the areas and controller design was done.

4. Simulation results

Area 1

Fig. 4 shows the singular value plot of Area 1 with controller. It shows that the loop-gain enables good performance as far as reference tracking and disturbance rejection are concerned. In the lower half of fig. 4, the singular value plot of open-loop gain is approximately the same as reciprocal of singular value plot of sensitivity function and in the lower half (below 0 dB line) the singular value plot of complementary sensitivity function matches that of the open-loop gain with controller. This is expected because sensitivity function becomes approximately equal to the inverse of open-loop gain with controller for values of maximum singular value of open-loop gain with controller >> 1. Also, if minimum singular value of open-loop gain with controller is << 1, the complementary sensitivity function approximately equals the open-loop gain with

controller. The controller transfer function designed for Area 1 is given in (17). Fig. 5 shows the open loop and closed loop step responses of area 1. The controller transfer function for Area 1 is given below.

8.002e08 s^9 + 9.856e12 s^8 + 4.056e16 s^7 + 5.614e19 s^6 + 1.58e21 s^5 + 1.456e22 s^4 + 5.618e22 s^3 + 1.605e23 s^2 + 2.693e23 s + 1.098e23 / (s^10 + 2.459e04 s^9 + 2.521e08 s^8 + 1.378e12 s^7 + 4.244e15 s^6 + 6.984e18 s^5 + 4.828e21 s^4 + 6.725e22 s^3 + 1.852e23 s^2 + 1.099e23 s)

(17)

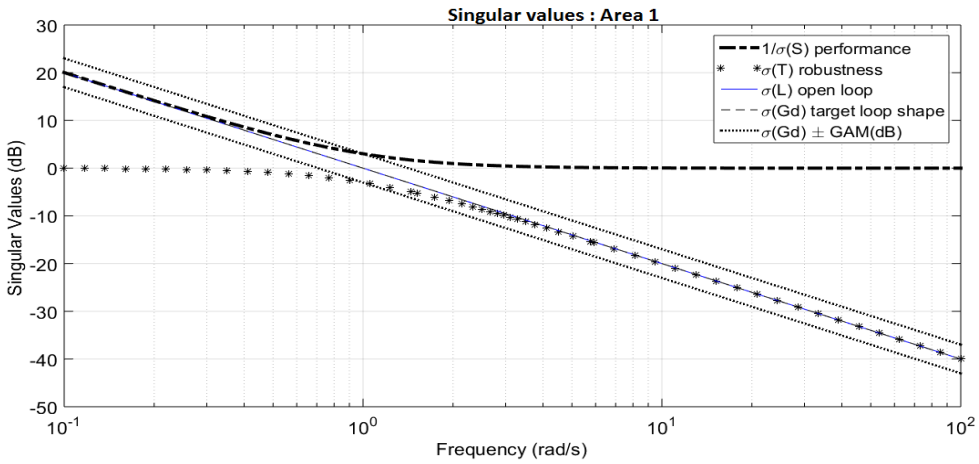

Fig. 4. Singular value plot of Area 1 with controller

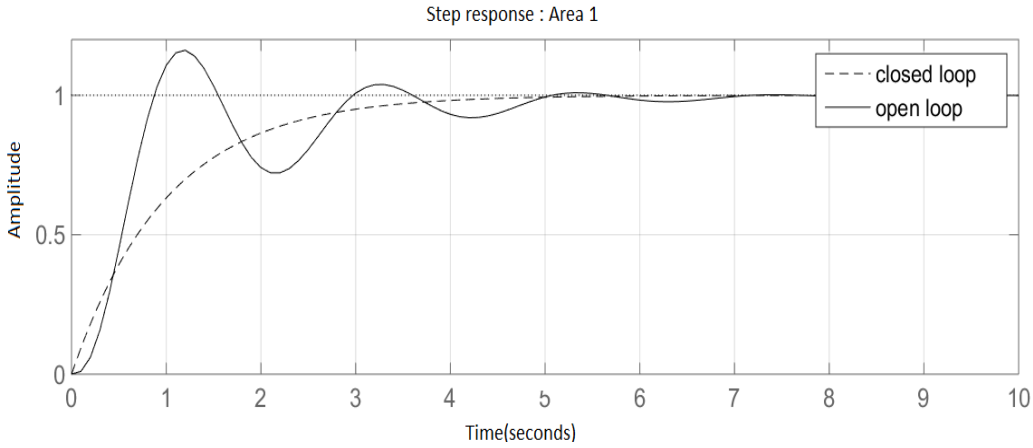

Fig. 5. Step response of Area 1

The value of γ for this controller was 1.4149. This shows the accuracy factor within which the designed controller has approached the desired loop gain.

Area 2

Fig. 6 shows the singular value plot of Area 2 with controller. It shows that the loop-gain is sufficient to give good performance as far as reference tracking and disturbance rejections are

concerned. It shows that the performance is good for low frequencies (indicated by inverse Singular Value Plot of sensitivity function) and offers good robustness at high frequencies as is indicated by the singular value plot of complementary sensitivity function. The controller transfer function designed for Area 2 is given in (18). Fig. 7 shows the open loop and closed loop step responses of Area 2. The controller transfer function for Area 2 is given below.

1.061e09 s^9 + 1.307e13 s^8 + 5.379e16 s^7 + 7.451e19 s^6 + 2.2e21 s^5 + 2.118e22 s^4 + 8.009e22 s^3 + 2.016e23 s^2 + 3.137e23 s + 1.331e23 /(s^10 + 2.459e04 s^9 + 2.521e08 s^8 + 1.379e12 s^7 + 4.246e15 s^6 + 6.991e18 s^5 + 4.838e21 s^4 + 7.475e22 s^3 + 2.125e23 s^2 + 1.333e23 s) (18)

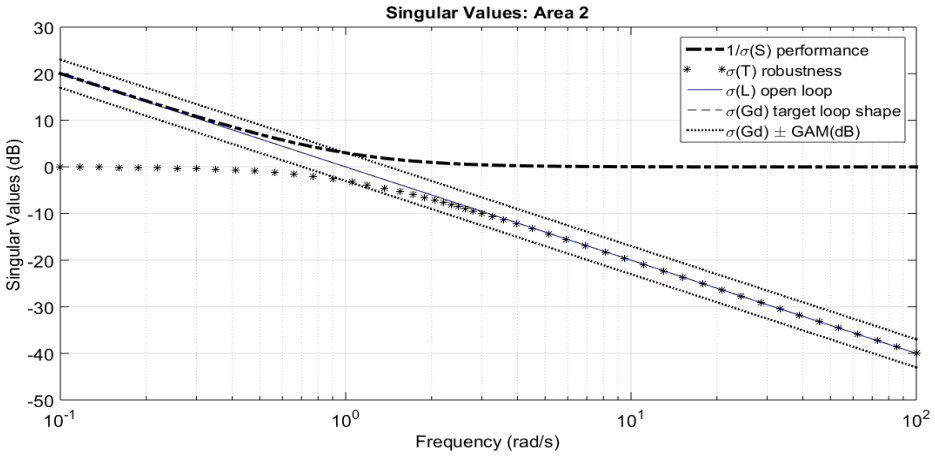

Fig. 6: Singular value plot of Area 2 with controller

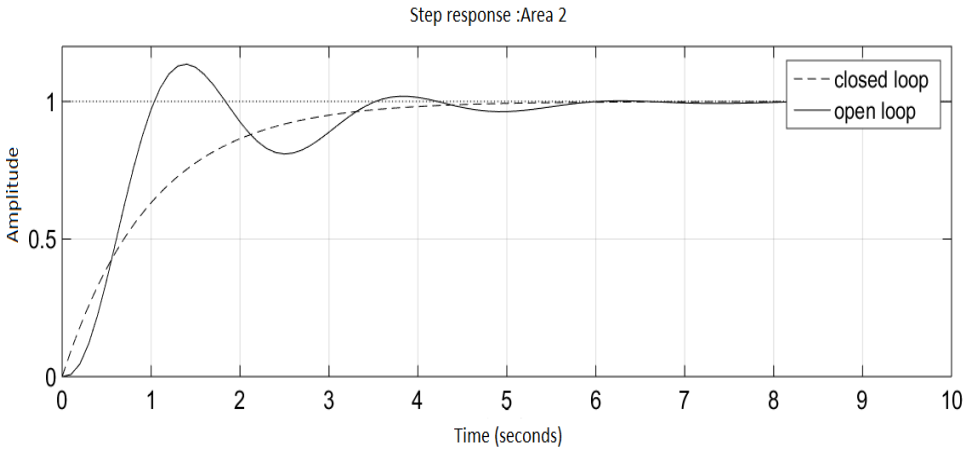

Fig. 7 Step response of Area 2

The value of γ for this controller was 1.414. This shows the accuracy factor within which the loop-gain using the designed controller has approached the desired loop gain. The tracking

performance of the system was observed using unit step command and the response showed good performance.

Dynamic performance of the system : 3 contract cases

The loop shaping controllers designed for the two areas were applied for LFC in a deregulated power system shown in fig. 1. The system parameters are given in Appendix A. The GENCOs are assumed to be of non-reheat thermal type. The three contract cases of operation in a deregulated power system were analyzed for the nominal plant and compared with the cases of uncertain plants which have +/-50% uncertainty for the significantly varying parameters like K_{p1}, K_{p2}, T_{p1}, T_{p2}, B_1, B_2 and T_{12}. The DPM used in the simulations for the three contract cases of operation is given in Appendix C. 'A' corresponds to uncertainty of +50%, 'B' corresponds to nominal plant performance and 'C' corresponds to uncertainty of -50% in all the simulation results. AGC is considered to have a time range from seconds to a few minutes, hence a time scale of 30 s is used for simulation.

Case 1- Unilateral contract (Poolco type)

In this type, DISCOs in an area have contract of power with GENCOs of the same area only. The computed values of steady state value of deviation in power generation of GENCO 1 and GENCO 2 are 0.1 pu MW each while that of GENCO 3 and GENCO 4 are zero as per (3). The corresponding frequency deviation for the two areas is shown in Fig. 8 and deviation in power generation of GENCO 1 and GENCO 2 are given in fig. 9 and that of GENCO 3 and GENCO 4 are given in fig. 10.

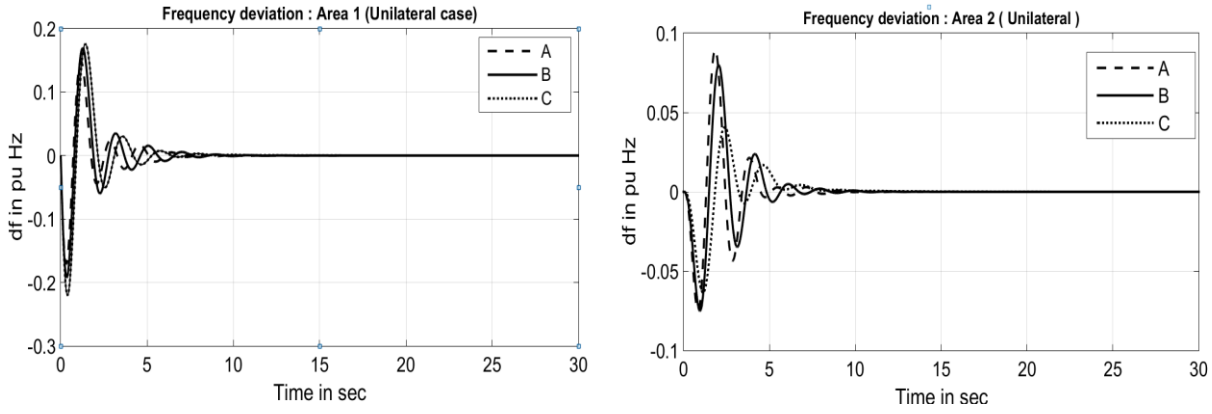

Fig. 8. Frequency deviation corresponding to Unilateral contract (a) Area 1 (b) Area 2;[Case A : Uncertainty +50%; Case B : Nominal Plant; Case C : Uncertainty -50%]

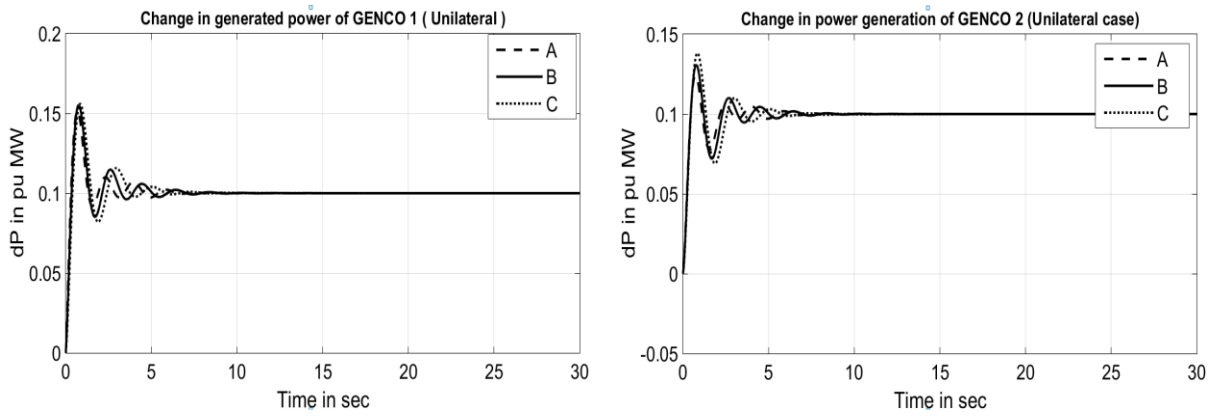

Fig. 9. Deviation in power generation corresponding to Unilateral contract (a) GENCO 1 (b) GENCO 2;[Case A : Uncertainty +50%; Case B : Nominal Plant; Case C : Uncertainty -50%]

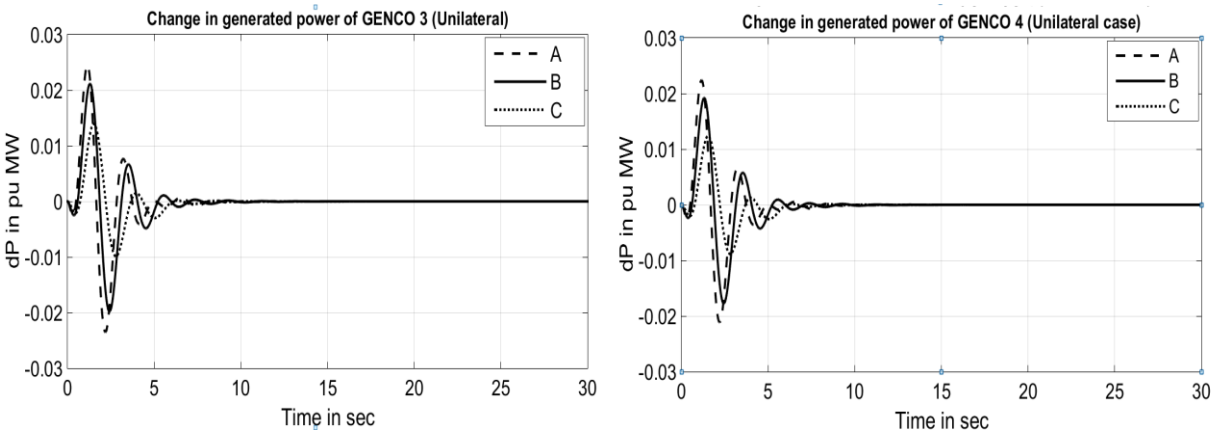

Fig. 10. Deviation in power generation corresponding to Unilateral contract (a) GENCO 3 (b) GENCO 4;[Case A : Uncertainty +50%; Case B : Nominal Plant; Case C : Uncertainty -50%]

Case 2 – Bilateral contract

In this type of contract, a DISCO makes contract for power with GENCOs in any control area. Referring to the DPM mentioned in Appendix C, the steady state values of deviation in power generation of GENCO 1 is 0.105 pu MW, that of GENCO 2 is 0.045 pu MW, GENCO 3 is 0.195 pu MW and of GENCO 4 is 0.055 pu MW. The corresponding frequency deviation for the two areas is shown in Fig. 11 and deviation in power generation of GENCO 1 and GENCO 2 are given in Fig. 12 and that of GENCO 3 and GENCO 4 are given in Fig. 13.

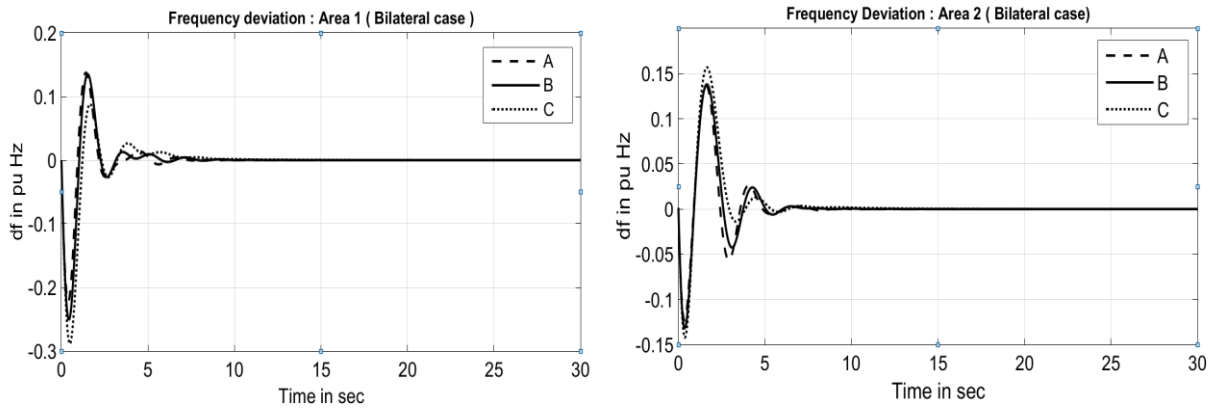

Fig. 11. Frequency deviation corresponding to bilateral contract (a) Area 1 (b) Area 2;[Case A : Uncertainty +50%; Case B : Nominal Plant; Case C : Uncertainty -50%]

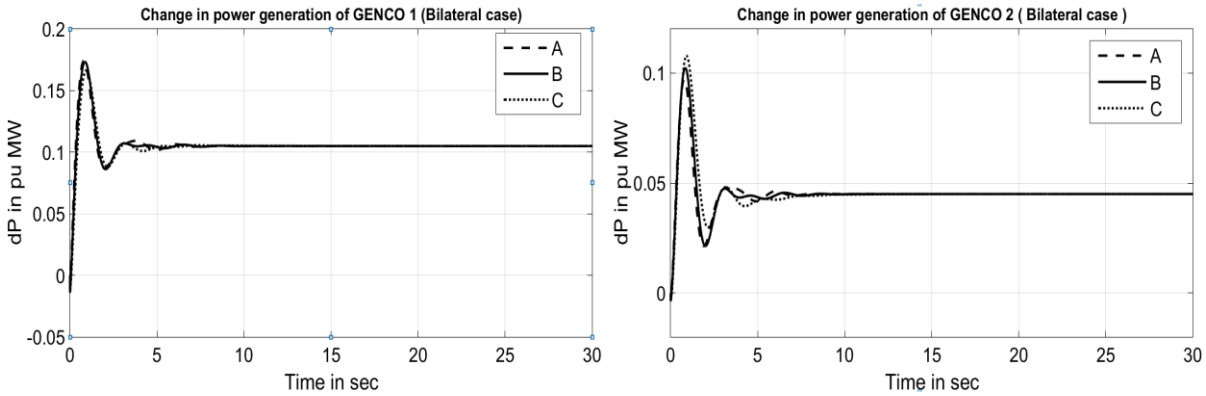

Fig. 12. Deviation in power generation corresponding to bilateral contract (a) GENCO 1 (b) GENCO 2;[Case A : Uncertainty +50%; Case B : Nominal Plant; Case C : Uncertainty -50%]

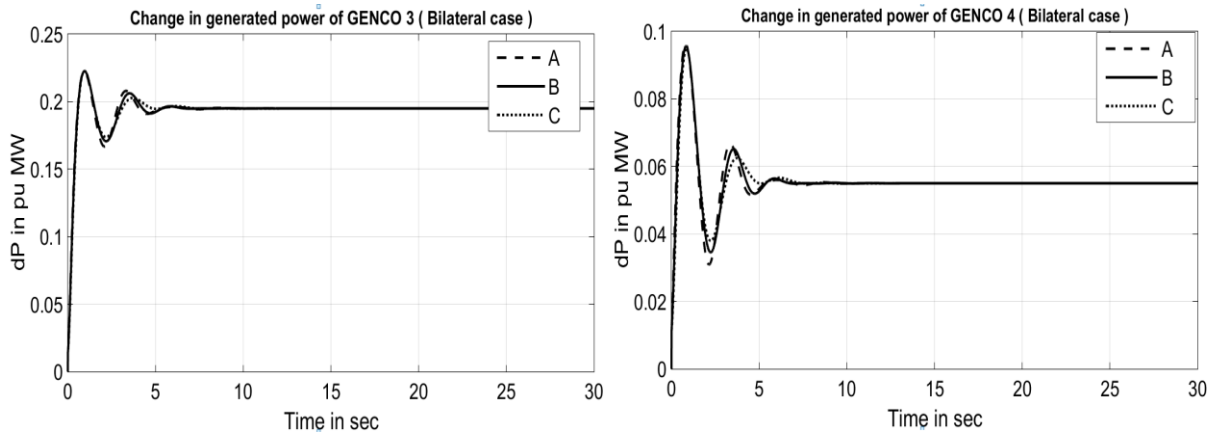

Fig. 13. Deviation in power generation corresponding to bilateral contract (a) GENCO 3 (b) GENCO 4;[Case A : Uncertainty +50%; Case B : Nominal Plant; Case C : Uncertainty -50%]

Case 3 – Contract violation

In certain situations, a DISCO may violate a contract by demanding excess power. This uncontracted power must be supplied by the GENCOs belonging to the same area where there is excess demand. In the simulation corresponding to contract violation, an excess of 0.1 pu MW is assumed occurring in the first area. Thus the computed steady state values of deviation in power generation of GENCO 1 becomes 0.18 pu MW, that of GENCO 2 is 0.07 pu MW, while that of G ENCOs 3 and 4 remain the same as in Case 2. The corresponding frequency deviation for the two areas is shown in fig. 14 and deviation in power generation of GENCO 1 and GENCO 2 are given in fig. 15 and that of GENCO 3 and GENCO 4 are given in fig. 16.

The change in tie-line power error corresponding to the three contract cases is given in fig. 17.

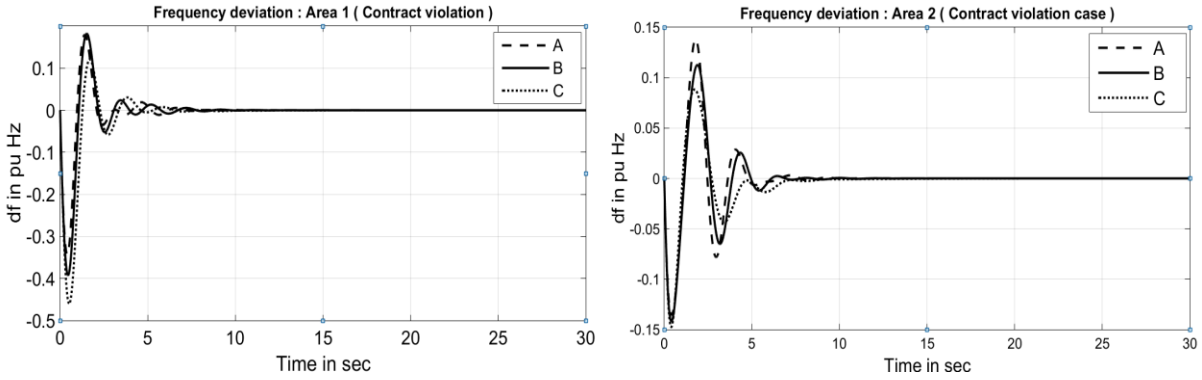

Fig. 14. Frequency deviation corresponding to contract violation (a) Area 1 (b) Area 2;[Case A : Uncertainty +50%; Case B : Nominal Plant; Case C : Uncertainty -50%]

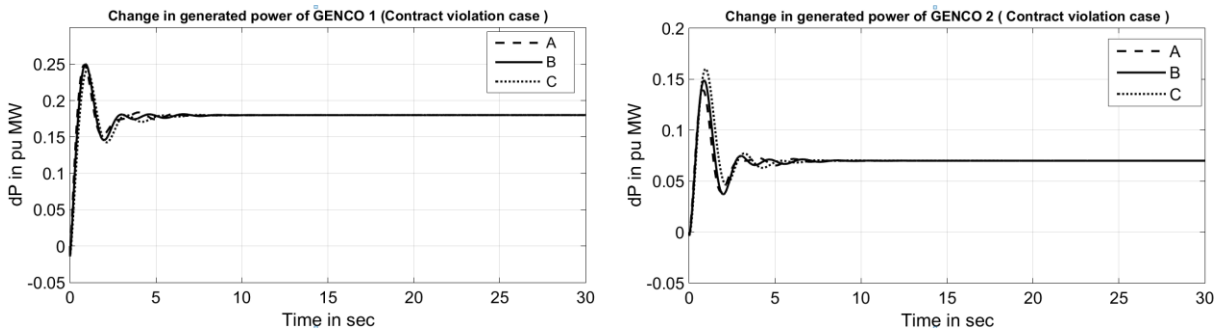

Fig. 15. Deviation in power generation corresponding to contract violation (a) GENCO 1 (b) GENCO 2;[Case A : Uncertainty +50%; Case B : Nominal Plant; Case C : Uncertainty -50%]

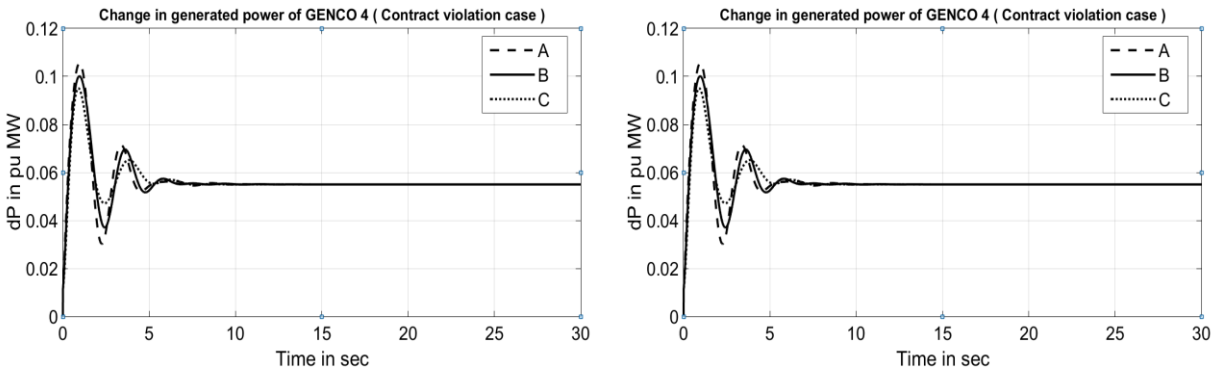

Fig. 16. Deviation in power generation corresponding to contract violation (a) GENCO 3 (b) GENCO 4;[Case A : Uncertainty +50%; Case B : Nominal Plant; Case C : Uncertainty -50%]

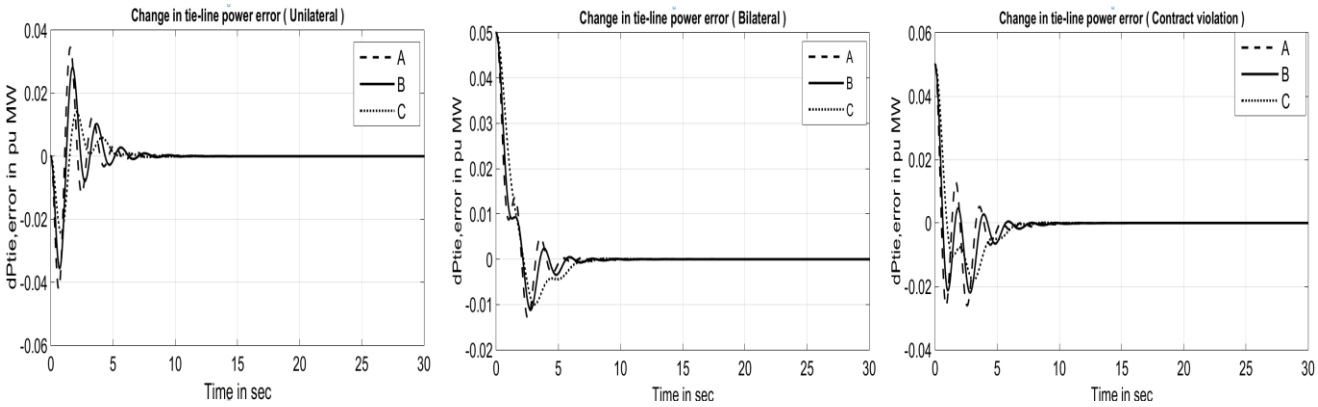

Fig. 17. Deviation in tie-line power error corresponding to (a) Unilateral (b) Bilateral (c) Contract violation;[Case A : Uncertainty +50%; Case B : Nominal Plant; Case C : Uncertainty -50%]

System behaviour towards cost functions

To compare the performance of the simulation results obtained, three performance indices of IAE (Integral Absolute Error), ISE (Integral Square Error) and ITAE (Integral Time Absolute Error) of the two control areas were computed for the three contract cases of unilateral, bilateral and contract violation cases. Here the error used is 'Area Control Error (ACE)' of the two areas and the observations are tabulated in Table 1. The DPM used for the three contract cases is given in Appendix C.

$$\text{IAE} = \int_0^t ACE_i \, dt \tag{19}$$

$$\text{ISE} = \int_0^t ACE_i^{\,2} \, dt \tag{20}$$

$$\text{ITAE} = \int_0^t t.|ACE_i| \, dt \tag{21}$$

Table 1. Performance indices for H-infinity controller for Area 1 and Area 2

		Unilateral	Bilateral	Contract violation
	Performance Index	H_∞	H_∞	H_∞
	NOMINAL PLANT			
Area 1	IAE	0.1848	0.1479	0.2434
	ISE	0.0127	0.0088	0.0258
	ITAE	0.3073	0.2259	0.3563
Area 2	IAE	0.0651	0.1600	0.1597
	ISE	0.0010	0.0092	0.0081
	UNCERTAIN PLANT (+50%)			
		Unilateral	Bilateral	Contract violation
Area 1	IAE	0.2202	0.2127	0.3151
	ISE	0.0202	0.0186	0.0462
	ITAE	0.3357	0.3208	0.4282
Area 2	IAE	0.0940	0.2156	0.2260
	ISE	0.0026	0.0153	0.0156
	ITAE	0.2303	0.3648	0.4193
	UNCERTAIN PLANT (-50%)			
Area 1	IAE	0.1034	0.0702	0.1304
	ISE	0.0042	0.0016	0.0067
	ITAE	0.1670	0.1439	0.2235
Area 2	IAE	0.0287	0.1185	0.1070
	ISE	0.0002	0.0048	0.0042
	ITAE	0.0729	0.2113	0.1681

5. Conclusions and future scope

In this paper a decentralized H-infinity loop-shaping controller is proposed for a two-area deregulated non-reheat thermal power system. The simulation results show that the closed loop performance objectives are achieved by loop-shaping the open-loop gain. These include good performance with respect to reference tracking and disturbance rejection at low frequencies and robustness against uncertainty especially at high frequencies. It is noteworthy that robust stabilization can be done without the need of frequency weighting as in conventional H-infinity

controller design. Also, control is achieved without explicitly considering phase information of the nominal plant.

From the dynamic performance analysis of the three contract cases, the frequency deviation plots give the desired results. Also the steady state values of deviation in power generation are same as the computed values for all the three contract cases. Thus the controllers designed for the two areas perform well, both for the nominal plant as well as for the uncertainty cases of +50% and -50%. All the three performance indices indicate that this control strategy is a good control scheme for LFC problem in *uncertain* deregulated power systems.

The controller designed being of higher order has disadvantages as far as implementation is concerned. Hence an alternate robust controller which is of lower order would be preferred and future work may be pursued in this direction.

Appendix A

System Data

$Kp_1 = Kp_2 = 127.5$ Hz / pu MW
$Tp_1 = 25$ s; $Tp_2 = 31.25$ s
$R_1 = 3$ Hz/ pu MW; $R_2 = 3.125$ Hz / pu MW;
$R_3 = 3.125$ Hz / pu MW; $R_4 = 3.375$ Hz / pu MW
$B_1 = 0.532$; $B_2 = 0.495$
$Tg_1 = 0.075$ s; $Tg_2 = 0.1$ s; $Tg_3 = 0.075$ s;
$Tg_4 = 0.0875$ s
$Tt_1 = 0.4$ s; $Tt_2 = 0.375$ s; $Tt_3 = 0.375$ s;
$Tt_4 = 0.4$ s

Appendix B

State Space Model :

First Area

$$A_1=\begin{bmatrix} -0.04 & -5.1 & 5.1 & 0 & 5.1 & 0 \\ 0.44 & 0 & 0 & 0 & 0 & 0 \\ 0 & 0 & -2.5 & 2.5 & 0 & 0 \\ -4.44 & 0 & 0 & -13.33 & 0 & 0 \\ 0 & 0 & 0 & 0 & -2.67 & 2.67 \\ -3.2 & 0 & 0 & 0 & 0 & -10 \end{bmatrix}; B_{11} = \begin{bmatrix} -5.1 & 0 & 0 & 0 & 0 \\ 0 & -1 & 0 & 0 & 0 \\ 0 & 0 & 0 & 0 & 0 \\ 0 & 0 & 0 & 13.33 & 0 \\ 0 & 0 & 0 & 0 & 0 \\ 0 & 0 & 0 & 0 & 10 \end{bmatrix}; B_{21} = \begin{bmatrix} 0 \\ 0 \\ 0 \\ 10 \\ 0 \\ 2.5 \end{bmatrix}; C_1 = [0.532 \quad 1 \quad 0 \quad 0 \quad 0 \quad 0]$$

;

$D_{1w}=[0 \quad 0 \quad -1 \quad 0 \quad 0]$

Second Area

$$A_2 = \begin{bmatrix} -0.03 & -4.08 & 4.08 & 0 & 4.08 & 0 \\ 0.44 & 0 & 0 & 0 & 0 & 0 \\ 0 & 0 & -2.67 & 2.67 & 0 & 0 \\ -4.27 & 0 & 0 & -13.33 & 0 & 0 \\ 0 & 0 & 0 & 0 & -2.5 & 2.5 \\ -3.39 & 0 & 0 & 0 & 0 & -11.43 \end{bmatrix}; B_{12} = \begin{bmatrix} -4.08 & 0 & 0 & 0 & 0 \\ 0 & -1 & 0 & 0 & 0 \\ 0 & 0 & 0 & 0 & 0 \\ 0 & 0 & 0 & 13.33 & 0 \\ 0 & 0 & 0 & 0 & 0 \\ 0 & 0 & 0 & 0 & 11.43 \end{bmatrix};$$

$$B_{22} = \begin{bmatrix} 0 \\ 0 \\ 0 \\ 6.67 \\ 0 \\ -5.714 \end{bmatrix}; \quad C_2 = [0.495 \quad 1 \quad 0 \quad 0 \quad 0 \quad 0]; ; D_{2w} = [0 \quad 0 \quad 1 \quad 0 \quad 0]$$

Appendix C

	Unilateral	Bilateral	Contract violation
DPM	$\begin{bmatrix} 0.6 & 0.4 & 0 & 0 \\ 0.4 & 0.6 & 0 & 0 \\ 0 & 0 & 0 & 0 \\ 0 & 0 & 0 & 0 \end{bmatrix}$	$\begin{bmatrix} 0.5 & 0.25 & 0 & 0.3 \\ 0.2 & 0.25 & 0 & 0 \\ 0 & 0.25 & 1 & 0.7 \\ 0.3 & 0.25 & 0 & 0 \end{bmatrix}$	$\begin{bmatrix} 0.5 & 0.25 & 0 & 0.3 \\ 0.2 & 0.25 & 0 & 0 \\ 0 & 0.25 & 1 & 0.7 \\ 0.3 & 0.25 & 0 & 0 \end{bmatrix}$

References

1. Kundur P "Power System Stability and Control," Mc Graw Hill, 2003 Edn.
2. Hassan Bevrani "Robust Power System Frequency Control," Springer, 2011 Edn.
3. Richard D Christie, Anjan Bose "Load Frequency control Issues in Power System Operations After Deregulation," IEEE Transactions on Power systems, Vol.11, No.3, pp. 1191-1200, August 1996
4. Bjorn H Bakken, Ove S Grande "Automatic Generation Control in a Power System," IEEE Trans. On Power Systems, Vol.13, No.4, November 1998
5. Vaibhav Donde, M A Pai, Ian A Hiskens "Simulation and Optimization in AGC Systems after deregulation," IEEE Transactions on Power Systems, Vol.16, No.3, August 2001
6. Bevrani H, Mitani Y, Tsuji K "Bilateral based robust load frequency control," Energy Conversion and Management, Vol.57, pp. 2297-2312, 2004
7. Shayeghi H, Shayanfar H A,O P Malik "Robust decentralized neural networks based LFC in a deregulated power system," Electric Power systems Research, Vol. 77, pp. 241-251, 2007
8. Demiroren A, Zeynelgil H L "GA application to optimization of AGC in three-area power system after deregulation," Electrical Power and Energy Systems, Vol. 29, pp. 230-240, 2007
9. Thottungal R, Anbalagan P "On fuzzy load frequency control in interconnected restructured power system with indeterministic load", Advances in Modelling Series C, Vol. 62, Issue 2, pp. 51-65, 2007
10. Praghnesh Bhatt, Ranjit Roy, S P Ghoshal "Optimized multi area AGC simulation in restructured Power systems," Electrical Power and Energy Systems, Vol. 32, pp. 311-322, 2010
11. Elyas Rakhshani, Javad Sadeh "Practical viewpoints on load frequency control problem in a deregulated power system," Energy Conversion and Management, Vol. 51, pp.1148-1156, 2010

12. Wen Tan, Hongxia Zhang , Mei Yu "Decentralized load frequency control in deregulated environments," Electrical Power and Energy Systems, Vol. 41, pp. 16-26, 2012

13. Wen Tan, Hong Zhou "Robust analysis of decentralised load frequency control for multi-area power systems, " Electrical Power and Energy Systems, Vol. 43,pp. 996-1005, 2012

14. Sanjoy Debbarma, Lalit Chandra Saikia, Nidul Sinha "AGC of a multi-area thermal system under deregulated environment using a non-integer controller," Electric Power Systems Research, Vol. 95, pp. 175-183, 2013

15. K P Singh Parmar, S Majhi, D P Kothari "LFC of an interconnected power system with multi-source power generation in deregulated power environment," Electrical Power and Energy Systems, Vol. 57, pp. 277-286, 2014

16. Le, V.X., and M.G. Safonov "Rational matrix GCD's and the design of squaring-down compensators—a state space theory," IEEE Trans. Autom. Control, Vol. 363, No.3, pp. 384–392, March 1992.

17. Glover, K., and D. McFarlane "Robust stabilization of normalized coprime factor plant descriptions with H_∞-bounded uncertainty," IEEE Trans. Automatic Control, Vol. 34, No. 8, pp. 821–830, August 1992

18. Chiang, R.Y., and M.G. Safonov "H∞ synthesis using a bilinear pole-shifting transform, AIAA J. Guidance, Control and Dynamics," Vol. 15, No.5, pp. 1111–1115, September–October 1992

19. Zhou, K., and J. C. Doyle "Essentials of Robust Control," NY: Prentice-Hall, 1998

20. Arlene Davidson R, S. Ushakumari "Optimal Load Frequency Controller for a Deregulated Non-Reheat Thermal Power System," Proceedings of the IEEE International Conference on Control, Computing and Communication ICCC 2015, pp. 319-324.

21. Arlene Davidson R, S. Ushakumari "H-Infinity Loop-Shaping Controller for Load Frequency Control of an Uncertain Deregulated Power System," Proceedings of the IEEE International Conference on Electrical, Electronics and Optimization Techniques ICEEOT 2016, Chennai, pp. 2185-2191.

22. Robust Control Toolbox, Matlab R 2015b